J|A|C|S
ARTICLES
Published on Web 12/29/2006

Near-Infrared (NIR) to Red and Green Up-Conversion Emission from Silica Sol−Gel Thin Films Made with $La_{0.45}Yb_{0.50}Er_{0.05}F_3$ Nanoparticles, Hetero-Looping-Enhanced Energy Transfer (Hetero-LEET): A New Up-Conversion Process

Sri Sivakumar,[†] Frank C. J. M van Veggel,*[,†] and P. Stanley May*[,‡]

Contribution from the Department of Chemistry, University of Victoria, P.O. Box 3065, Victoria, British Columbia, Canada V8W 3V6, and Chemistry Department, University of South Dakota, 414 East Clark Street, Vermillion, South Dakota 57069

Received July 26, 2006; E-mail: fvv@uvic.ca; stanley.may@usd.edu

Abstract: Bright green and red luminescence has been generated with a 980 nm diode laser from silica sol−gel thin films made with $La_{0.45}Yb_{0.50}Er_{0.05}F_3$ nanoparticles through a newly described hetero-looping-enhanced energy-transfer (hetero-LEET) up-conversion process, which exhibits a power dependence *similar* to that of a photon avalanche (PA). The hetero-LEET mechanism is potentially more efficient than PA, ground-state absorption/excited-state absorption (GSA/ESA), and energy-transfer (ETU) mechanisms because it combines resonant ground-state absorption with a looping or feedback process.

Introduction

Lanthanide-based up-conversion phosphors are being investigated for a wide range of potential applications, such as display monitors, fluorescence imaging for detection of biomolecules, optical data storage, LCD back lighting, and compact solid-state lasers.[1−6] Research in this area has greatly intensified due to the recent development of lanthanide-doped oxide[3,5,7−11] and fluoride nanoparticles[12−15] that exhibit NIR-to-visible up-conversion emission. Nanocrystalline up-conversion phosphors can be incorporated into a broad range of materials and devices and are suitable for sensing at the molecular scale. At present, low efficiency is the most important limiting factor in the practical use of up-conversion phosphors.[16] Up-conversion luminescence occurs via three basic mechanisms (Figure 1): (A) ground-state absorption followed by excited-state absorption (GSA/ESA); (B) sequential energy-transfer events from donors to the up-converting acceptor (ETU);[17] and (C) photon avalanche (PA).[17−20] In the PA mechanism, the intermediate reservoir level is initially populated through a very weak ground-state absorption, followed by resonant excited-state absorption (ESA) or energy transfer from another excited ion, to populate the upper level from which up-conversion luminescence occurs. After this initial "seeding" process, efficient cross-relaxation (CR) populates the reservoir levels of neighboring ions to produce two ions in the key reservoir level. A feedback, or "looping", cycle of ESA (or energy transfer) followed by cross-relaxation then

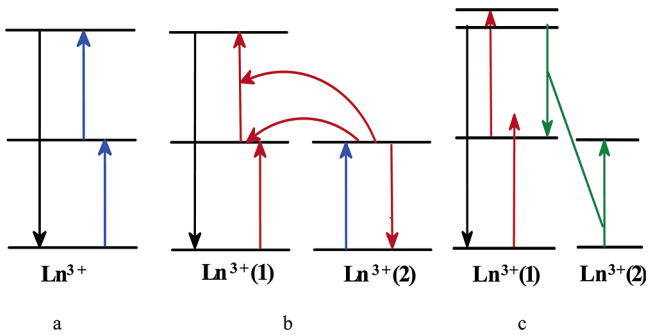

Figure 1. Schematic diagram of classical up-conversion mechanisms: (a) ground-state absorption/excited-state absorption (GSA/ESA), (b) energy-transfer up-conversion (ETU), (c) photon avalanche (PA).

[†] University of Victoria.
[‡] University of South Dakota. On sabbatical leave at University of Victoria.

(1) Lim, S. F.; Riehn, R.; Ryu, W. S.; Khanarian, N.; Tung, C. K.; Tank, D.; Austin, R. H. *Nano Lett.* **2006**, *6*, 169.
(2) Mehta, A.; Thundat, T.; Barnes, M. D.; Chhabra, V.; Bhargava, R.; Bartko, A. P.; Dickson, R. M. *Appl. Opt.* **2003**, *42*, 2132.
(3) Zhang, H. X.; Kam, C. H.; Zhou, Y.; Han, X. Q.; Buddhudu, S.; Xiang, Q.; Lam, Y. L.; Chan, Y. C. *Appl. Phys. Lett.* **2000**, *77*, 609.
(4) Soo, Y. L.; Huang, S. W.; Ming, Z. H.; Kao, Y. H.; Smith, G. C.; Goldburt, E.; Hodel, R.; Kulkarni, B.; Veliadis, J. V. D.; Bhargava, R. N. *J. Appl. Phys.* **1998**, *83*, 5404.
(5) Patra, A.; Friend, C. S.; Kapoor, R.; Prasad, P. N. *J. Phys. Chem. B* **2002**, *106*, 1909.
(6) Sivakumar, S.; Diamente, P. R.; van Veggel, F. C. J. M. *Chem.—Eur. J* **2006**, *12*, 5884.
(7) Heer, S.; Lehmann, O.; Haase, M.; Güdel, H. U. *Angew. Chem., Int. Ed.* **2003**, *42*, 3179.
(8) Patra, A.; Friend, C. S.; Kapoor, R.; Prasad, P. N. *Appl. Phys. Lett.* **2003**, *83*, 284.
(9) Vetrone, F.; Boyer, J. C.; Capobianco, J. A.; Speghini, A.; Bettinelli, M. *J. Phys. Chem. B* **2003**, *107*, 1107.
(10) Vetrone, F.; Boyer, J. C.; Capobianco, J. A.; Speghini, A.; Bettinelli, M. *Chem. Mater.* **2003**, *15*, 2737.
(11) Wang, X.; Kong, X. G.; Shan, G. Y.; Yu, Y.; Sun, Y. J.; Feng, L. Y.; Chao, K. F.; Lu, S. Z.; Li, Y. J. *J. Phys. Chem. B* **2004**, *108*, 18408.
(12) Heer, S.; Kompe, K.; Güdel, H. U.; Haase, M. *Adv. Mater.* **2004**, *16*, 2102.
(13) Stouwdam, J. W.; van Veggel, F. C. J. M. *Nano Lett.* **2002**, *2*, 733.
(14) Stouwdam, J. W.; van Veggel, F. C. J. M. *Langmuir* **2004**, *20*, 11763.
(15) Sudarsan, V.; Sivakumar, S.; van Veggel, F. C. J. M.; Raudsepp, M. *Chem. Mater.* **2005**, *17*, 4736.

10.1021/ja065378x CCC: $37.00

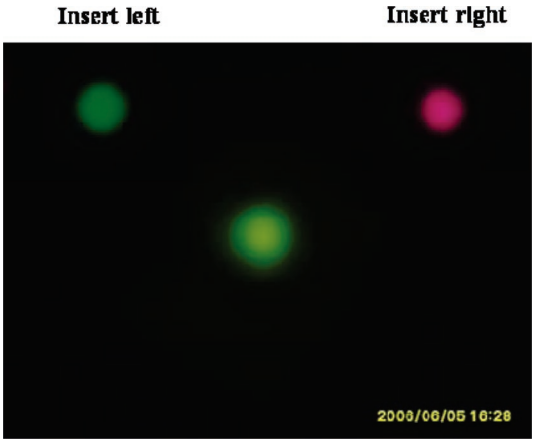

Figure 2. Digital photograph of up-conversion emission from silica sol−gel thin film prepared at 800 °C made with $La_{0.45}Yb_{0.50}Er_{0.05}F_3$ nanoparticles under 980 nm 4.5 W/cm^2 CW laser excitation (insert left is up-converted green emission by filtering red emission, and insert right is up-converted red emission by filtering green emission). Digital photographs were taken using an 800 nm low band-pass filter to shield 980 nm laser light from the camera.

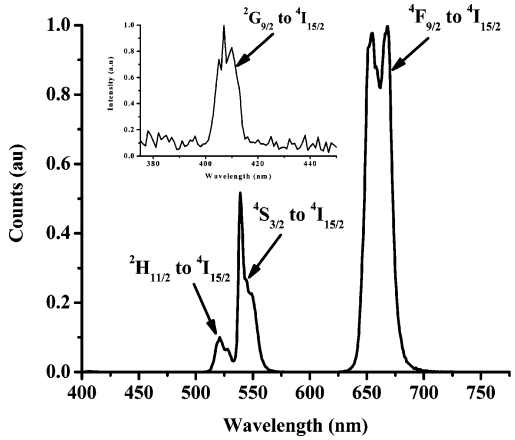

Figure 3. Up-conversion emission spectrum of silica thin film prepared at 800 °C made with $La_{0.45}Yb_{0.50}Er_{0.05}F_3$ nanoparticles under 980 nm 4.5 W/cm^2 CW laser excitation (inset is weak blue emission from the $^2G_{9/2}$ level of the Er^{3+} ion).

ensues, leading eventually to a substantial population of the reservoir level and, therefore, to strong up-conversion emission.

Although photon avalanche mechanisms can be relatively efficient, they suffer from a number of drawbacks. Maximum output is limited because of the weak ground-state absorption,[21] and high pump powers are usually needed to reach the threshold condition. In addition, because many looping cycles are required to achieve avalanche, the rise time in the temporal evolution of the up-conversion emission is generally much longer (up to seconds) than the lifetimes of any of the excited states involved, which can be a disadvantage in lighting and display applications.

We report here the efficient generation of bright green and red light through up-conversion of 980 nm light from silica sol−gel thin films made with $La_{0.45}Yb_{0.50}Er_{0.05}F_3$ nanoparticles at room temperature. This process occurs via a new, potentially

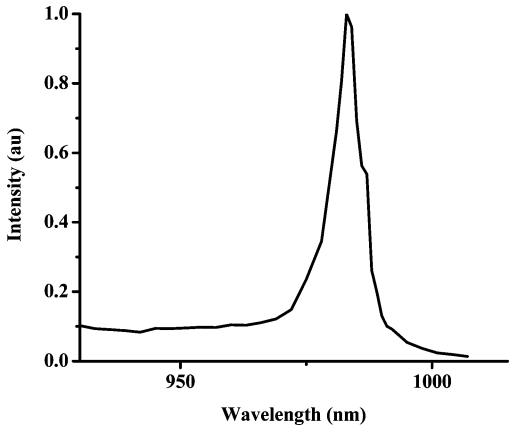

Figure 4. Excitation spectrum of silica thin film prepared at 800 °C made with $La_{0.45}Yb_{0.50}Er_{0.05}F_3$ nanoparticles (λ_{em} = 545 nm).

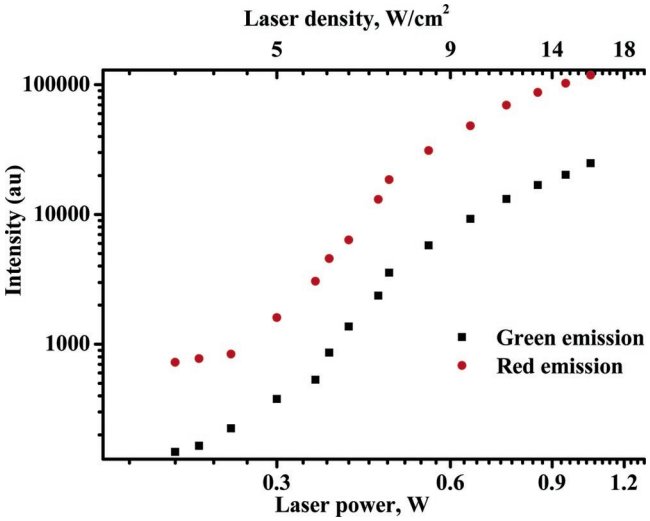

Figure 5. Dependence of the up-conversion emission intensity on 980 nm CW laser excitation power in silica thin film prepared at 800 °C made with $La_{0.45}Yb_{0.50}Er_{0.05}F_3$ nanoparticles (end of fiber is 8 mm away from the sample).

more efficient up-conversion mechanism, termed hetero-looping-enhanced energy-transfer (hetero-LEET) up-conversion. This mechanism combines the advantages of resonant ground-state absorption of the pump beam and an ETU-based up-conversion with a looping (feedback) mechanism that enhances the population of the reservoir levels. The dependence of up-conversion emission intensity on pump power is similar to that seen for a photon avalanche process, except that, due to non-negligible ground-state absorption, there is no manifestation of a distinct threshold condition for hetero-LEET. In addition, the rise time of up-conversion emission is only on the order of the lifetimes of the participating excited states of the Er^{3+} and Yb^{3+} ions. Up-conversion emission is easily seen by the naked eye at laser power densities of 4.5 W/cm^2 or less, even for dilute samples.

Goldner et al.[21] have demonstrated a cross-relaxation-enhanced GSA/ESA up-conversion mechanism, which they call CRESA, in a Nd^{3+}-doped $LiYF_4$ single crystal. They have demonstrated that CRESA is more efficient than the photon avalanche process because of the resonant GSA. However, CRESA has been described only in a single crystal and is based on the intrinsically less efficient GSA/ESA process. To the best of our knowledge, this is the first report on the generation of green and red emission from Er^{3+}-doped nanosized materials

(16) Suyver, J. F.; Aebischer, A.; Biner, D.; Gerner, P.; Grimm, J.; Heer, S.; Kramer, K. W.; Reinhard, C.; Güdel, H. U. *Opt. Mater.* **2005**, *27*, 1111.
(17) Scheps, R. *Prog. Quantum Electron.* **1996**, *20*, 271.
(18) Wright, J. C. *Top. Appl. Phys.* **1976**, *15*, 239.
(19) Joubert, M. F. *Opt. Mater.* **1999**, *11*, 181.
(20) Auzel, F. *Chem. Rev.* **2004**, *104*, 139.
(21) Goldner, P.; Pelle, F. *Opt. Mater.* **1996**, *5*, 239.

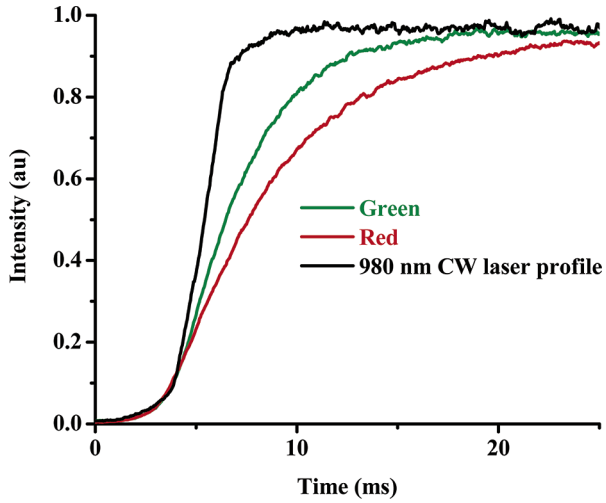

Figure 6. Temporal evolution of green emission through up-conversion from silica thin film prepared at 800 °C made with $La_{0.45}Yb_{0.50}Er_{0.05}F_3$ nanoparticles under 980 nm 4.5 W/cm^2 CW laser excitation (end of fiber is 8 mm away from the sample). The shape of graphs between 0 and 5 ms is a result of the low chopper speed and the finite size of the 980 nm laser light and has no physical meaning.

through a feedback process and is the first report of feedback enhancement of an ETU mechanism.

Experimental Section

All chemicals were used as received without further purification. The lanthanide salts, $La(NO_3)_3{\cdot}6H_2O$, $Er(NO_3)_3{\cdot}6H_2O$, $Lu(NO_3)_3{\cdot}5H_2O$, and $Yb(NO_3)_3{\cdot}5H_2O$, all having a purity of 99.99%, and tetraethylorthosilicate (TEOS) (99.99%), NH_4OH (35 wt % aqueous solution), and sodium fluoride (99%) were purchased from Aldrich. Citric acid (99%) was purchased from Caledon Laboratories Ltd. Approximately 2 g of citric acid and 0.126 g of NaF were dissolved in 40 mL of distilled water. The pH of the solution was adjusted to 6 by adding NH_4OH_{aq}, and the solution was heated to 75 °C. Stoichiometric amounts of the lanthanide nitrate salts were dissolved in 2 mL of methanol and added dropwise. A clear solution was obtained, and after 2 h of reaction, the mixture was cooled to room temperature. Subsequently, 70 mL of ethanol was added to the reaction mixture to precipitate the nanoparticles. The nanoparticles were collected by centrifugation at 3000 rpm, washed twice with 5 mL of ethanol, and dried at room temperature under vacuum. After drying, the particles can easily be dispersed in water. Formation of citrate-stabilized nanoparticles was confirmed from ^{1}H NMR and AFM studies which are consistent with our earlier reports.[6,15,22]

Ln^{3+}-doped LaF_3 nanoparticles (50 mg) were dispersed in 2 mL of water, after which the dispersion was mixed with 3 mL of tetraethylorthosilicate (TEOS) and 7.8 mL of ethanol. The pH of the solution was adjusted to 2 by adding a few drops of 0.1 N HCl, and the solution was stirred for 24 h to get a clear sol. The sol was then spin coated on a quartz substrate at 2500 rpm and heated to 400 °C from 25 °C in

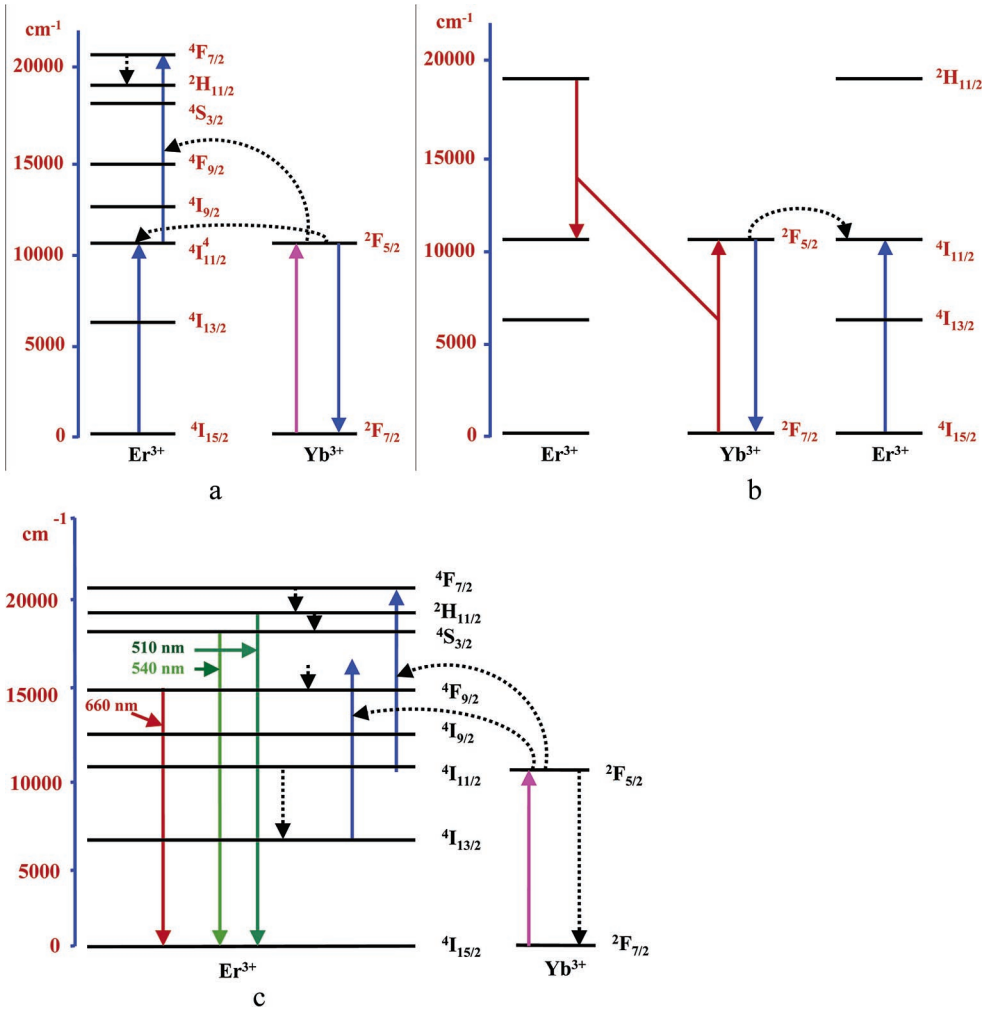

Figure 7. Up-conversion mechanism through the hetero-LEET process. (a) Initial stage involving ETU. (b) Start of feedback loop via Yb^{3+}-assisted $Er^{3+}-Er^{3+}$ cross-relaxation (some energy levels have been omitted for clarity). (c) Generation of red and green emission from Er^{3+}.

1.40 h, staying at 400 °C for 30 min and then heated to 800 °C in 2 h and staying at 800 °C for 12 h under ambient environment. The films were transparent to visible light, and no cracks were observed under an optical microscope. Our previous report[15] showed the presence of a nonstoichiometric lanthanum silicate phase ($La_{9.31}Si_{6.24}O_{26}$) along with the expected LaF_3 phase from X-ray diffraction (XRD) studies carried out on a silica thin film sample heated at 800 °C. Line width analysis showed that these phases are nanoparticles, embedded in a SiO_2 matrix.

Fluorescence analyses were done using an Edinburgh Instruments FLS 920 fluorescence system, which employs a photon-counting detection system using a cooled Hamamatsu R955 photomultiplier tube (PMT). For emission spectra, sample excitation was accomplished using a Coherent 2-pin 980 nm CW semiconductor diode laser (P_{max} = 800 mW at 1000 mA) coupled to a 100 μm (core) multimode optical fiber. All the emission analyses in the visible region were measured with a 1 nm resolution. Up-conversion excitation spectra were acquired using a Vibrant II OPO (Opotek) as an excitation source. All spectra were corrected for instrument sensitivity. The rise times of up-conversion emission were determined by chopping the 980 nm CW laser excitation with an optical chopper operated at 2.7 Hz and recording the time dependence of up-conversion by monitoring the PMT output with a digital storage oscilloscope. Following the onset of excitation, the time dependence of up-conversion emission, $I(t)$, could be well fitted to

$$I(t) = A(1 - e^{-t/\tau})$$

where τ is the rise time and A is an empirical scaling parameter.

Effective lifetimes were calculated using Origin software (version 7.0) based on the equation[23]

$$\tau_{eff} = \frac{\int_0^\infty tI(t)dt}{\int_0^\infty I(t)dt}$$

Intensities down to 1% of the initial intensities were included in these lifetime analyses.

For consistency, all the thin film materials were scratched from the quartz plate, 15 mg of which was mixed with 35 mg of KBr to make uniform pellets. The emission intensities over the whole area of the pellet were the same within experimental error. The power density was calculated based on the divergence of laser light (10°) and distance between the sample and laser. Intensities in the power dependence graphs were calculated based on the integrated area under the peaks of emission spectrum under respective power densities. Control samples of citrate-stabilized $La_{0.45}Lu_{0.50}Er_{0.05}F_3$ and $La_{0.90}Yb_{0.05}Er_{0.05}F_3$ nanoparticles were heated at 500 °C to burn off the citrate. The absence of the C=O stretch in the IR spectrum of these heated materials confirms that all the citrate had been burned off. XRD of these materials confirmed the presence of pure LaF_3 phase.

Results and Discussion

Figure 2 shows a digital image of up-converted light (under 980 nm CW laser excitation) from the silica thin film made with $La_{0.45}Yb_{0.50}Er_{0.05}F_3$ nanoparticles. Bright light (which is green in appearance) can be seen very clearly from the thin film even at a laser power density of 4.5 W/cm^2. The insert left in Figure 2 shows the digital image of bright up-converted green light by filtering the red light, and insert right shows bright up-converted red light by filtering the green light. The corresponding up-conversion emission spectrum is shown in Figure 3. The emission peaks at 515, 540, and 660 nm are assigned to the

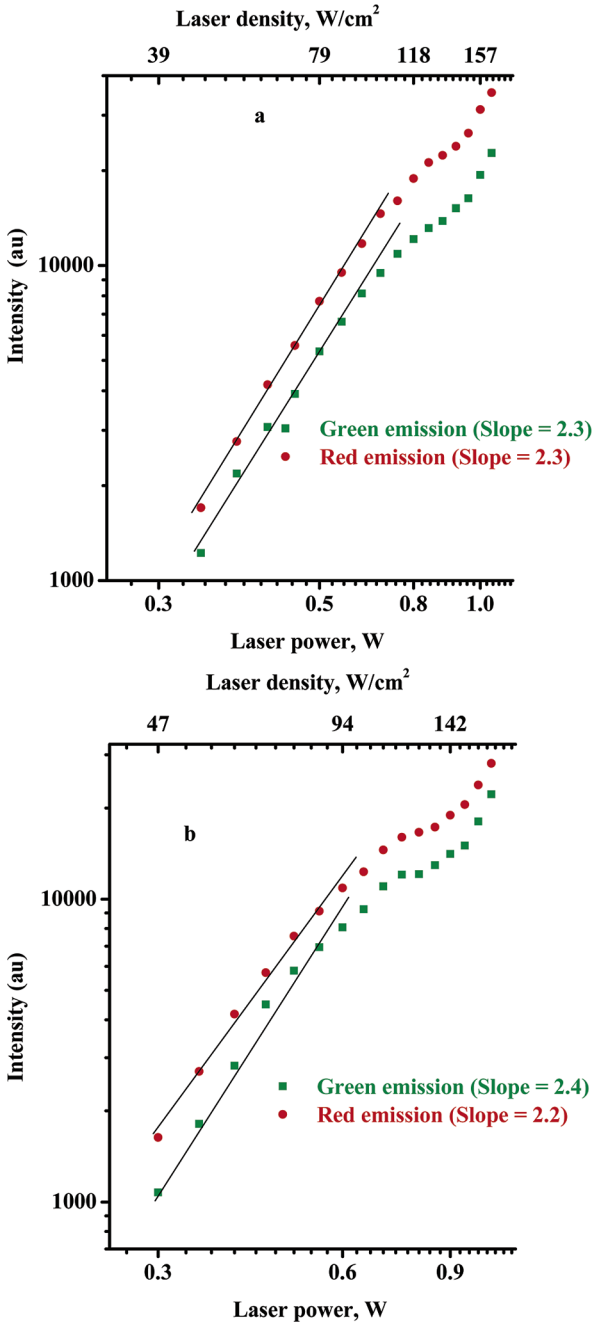

Figure 8. Dependence of the up-conversion emission intensity on the excitation power in silica thin films prepared at 800 °C made with (a) $La_{0.45}Lu_{0.50}Er_{0.05}F_3$ nanoparticles or (b) $La_{0.90}Yb_{0.05}Er_{0.05}F_3$ nanoparticles under 980 nm CW laser excitation (end of fiber is 3 mm away from the sample).

$^2H_{11/2} \rightarrow {}^4I_{15/2}$, $^4S_{3/2} \rightarrow {}^4I_{15/2}$, and $^4F_{9/2} \rightarrow {}^4I_{15/2}$ transitions of Er^{3+} ion, respectively.[24] Additionally, a very weak blue emission band at 410 nm was observed and has been assigned to Er^{3+}: $^2G_{9/2} \rightarrow {}^4I_{15/2}$ (inset in Figure 3).[24] The NIR excitation spectrum (Figure 4) of green up-conversion emission shows the typical absorption of Yb^{3+} ion, which clearly demonstrates that the up-conversion occurs from the Er^{3+} ion through energy transfer from Yb^{3+} to Er^{3+} ions (i.e., an ETU mechanism). The excitation spectrum of red up-conversion emission (not shown) is essentially identical to that of the green.

Figure 5 plots the up-conversion emission intensity versus the excitation power. At 4.5 W/cm^2 laser power density, the

(22) Sivakumar, S.; van Veggel, F. C. J. M.; Raudsepp, M. *J. Am. Chem. Soc.* **2005**, *127*, 12464.
(23) Cannas, C.; Casu, M.; Mainas, M.; Musinu, A.; Piccaluga, G.; Polizzi, S.; Speghini, A.; Bettinelli, M. *J. Mater. Chem.* **2003**, *13*, 3079.
(24) Stein, G.; Würzberg, E. *J. Chem. Phys.* **1975**, *62*, 208.

slopes of both the red and green emission increase rapidly with increasing excitation power, reaching a maximum slope of ~8. This is strong evidence for a feedback mechanism, as it is hard to envision an effective eight-photon process in this system that does not involve a repetitive feedback loop. Moreover, the nearly identical shapes of the red and green emission power dependence graphs above 4.5 W/cm^2 laser power density demonstrate that the same intermediate state reservoir is involved in both up-conversion processes. In our earlier report,[22] we had assigned the green and red emission to a two-photon process because we had only measured the emissions at higher laser densities (>60 W/cm^2), at which saturation effects are already apparent.

The temporal evolution (Figure 6) of red and green emission at the onset of 980 nm excitation exhibits rise times of 5.7 and 3.0 ms, respectively. These rise times are on the order of the lifetimes of the metastable levels $^4I_{11/2}$ and $^4I_{13/2}$ of Er^{3+} ions, respectively, and are considerably shorter than those typically observed in a PA mechanism. In addition, the rise time of red emission roughly matches the lifetime of the $^4I_{13/2}$ level of Er^{3+} and suggests that the $^4F_{9/2}$ emitting level is populated via the $^4I_{13/2}$ level.

The proposed mechanism of hetero-looping-enhanced energy-transfer up-conversion (hetero-LEET) responsible for both red and green emission is illustrated schematically in Figure 7. Initially, sequential energy transfers from $Yb^{3+}(^2F_{5/2})$ ions (excited by 980 nm light) result in an Er^{3+} ion in the $^4F_{7/2}$ excited state (Figure 7a). Then, through multiphonon-assisted relaxation, the $^2H_{11/2}$ level of Er^{3+} is populated. The energy difference of ~1200 cm^{-1} is easily taken up by 3−4 phonons of the LaF_3 phase or 1−2 phonons of the lanthanum silicate phase (see below). Figure 7b then illustrates the critical step that begins the feedback loop. Multiphonon-assisted cross-relaxation between $Er^{3+}(^2H_{11/2})$ and $Yb^{3+}(^2F_{7/2})$ ions results in excited $Er^{3+}(^4I_{11/2})$ and $Yb^{3+}(^2F_{5/2})$ ions. The energy difference of ~1100 cm^{-1} can easily be taken from 3 to 4 phonons of the LaF_3 phase or 1−2 phonons of the lanthanum silicate phase. The $Yb^{3+}(^2F_{5/2})$ ion then transfers its energy to a ground-state Er^{3+} ion to produce another $Er^{3+}(^4I_{11/2})$ ion. The net effect of the process illustrated in Figure 7b is, therefore, $Er^{3+}(^2H_{11/2}) + Er^{3+}(^4I_{15/2}) \rightarrow 2Er^{3+}(^4I_{11/2})$. (Note, then, that the role of Yb^{3+} at this stage in the mechanism is to facilitate $Er^{3+}-Er^{3+}$ cross-relaxation.) It is this step that provides the multiplier effect to produce $Er^{3+}(^4I_{11/2})$, which is the reservoir level for up-conversion. Feedback, or looping, occurs because energy transfer from the $Yb(^2F_{5/2})$ to $Er^{3+}(^4I_{11/2})$ ion regenerates $Er^{3+}(^2H_{11/2})$, which resets the loop. One has to bear in mind that the Yb^{3+} ion which is involved in the cross-relaxation in Figure 7b is (most likely) different from the Yb^{3+} ion involved in Figure 7a because of the high concentration of Yb^{3+}. This high Yb^{3+} concentration also facilitates energy migration between them. As a result, the high Yb^{3+} concentration makes the cross-relaxation between two Er^{3+} ions relatively efficient when compared to that of the other energy-transfer steps in Figure 7a and 7c.

Figure 7c shows the generation of up-conversion emission from within this loop. Green emission is generated by multiphonon relaxation from $Er^{3+}(^4F_{7/2})$ to $Er^{3+}(^2H_{11/2} + {}^4S_{3/2})$ level, followed by $Er^{3+}(^4S_{3/2}) \rightarrow Er^{3+}(^4I_{15/2})$ emission. For red emission, excited Er^{3+} ions in the $^4I_{11/2}$ reservoir level relax to the $^4I_{13/2}$ level through multiphonon relaxation. Immediately following this process, the excited $Er^{3+}(^4I_{13/2})$ ion is excited further to the $^4F_{9/2}$ level through energy transfer from excited Yb^{3+} ions. In the absence of looping, both red and green up-conversion should be two-photon processes. This is supported by the observed power dependence (slope ~ 2) of up-conversion intensity at low laser power densities (<4.5 W/cm^2), at which feedback amplification is unimportant.

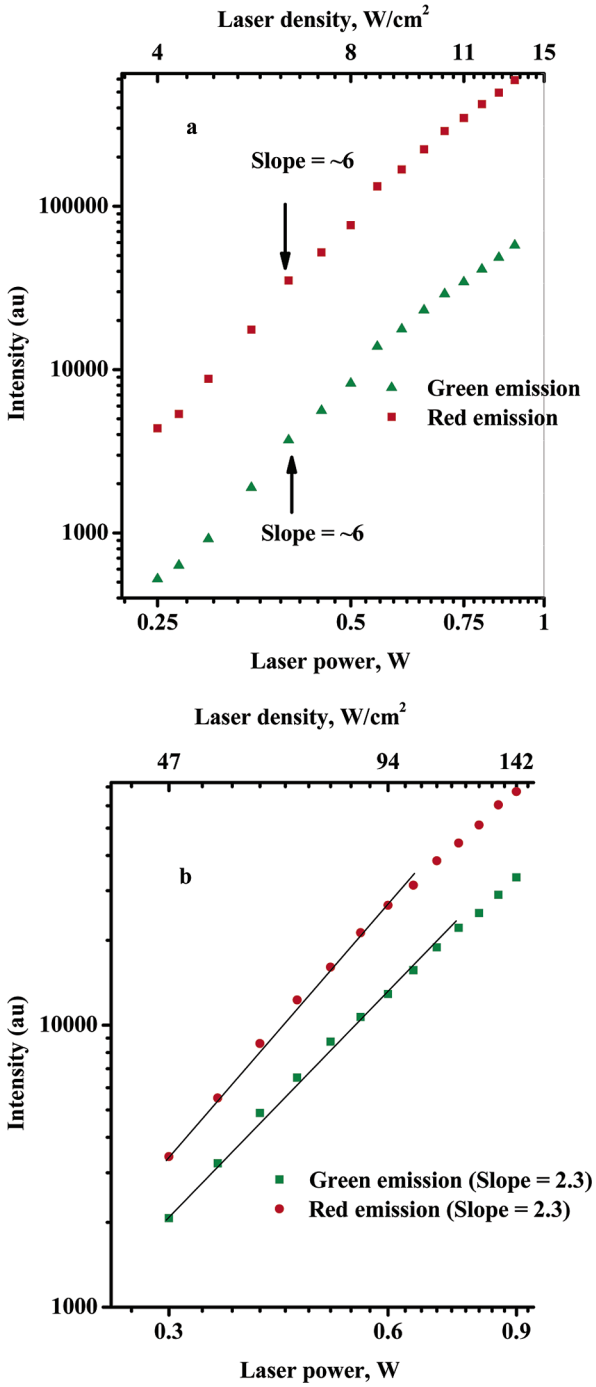

Figure 9. Dependence of the up-conversion emission intensity on the excitation power in heated (a) $La_{0.45}Yb_{0.50}Er_{0.05}F_3$ nanoparticles or (b) $La_{0.45}Lu_{0.50}Er_{0.05}F_3$ nanoparticles under 980 nm CW laser excitation (end of fiber is 3 mm away from the sample).

In order to investigate the importance of Yb^{3+} in the hetero-LEET mechanism, two control samples were prepared. Figure 8 shows the power dependence graphs of control silica thin films individually made with $La_{0.45}Lu_{0.50}Er_{0.05}F_3$ (no Yb^{3+} ion, Figure

8a) and $La_{0.90}Yb_{0.05}Er_{0.05}F_3$ nanoparticles (low Yb^{3+} ion concentration, Figure 8b), giving a slope of 2 over most of the power range. This clearly demonstrates that these are normal two-photon processes. Interestingly, however, they show the appearance of possible feedback contribution at higher laser densities, which suggests the possibility of a looping mechanism involving direct $Er^{3+}-Er^{3+}$ cross-relaxation. Nevertheless, direct $Er^{3+}-Er^{3+}$ cross-relaxation is unlikely to dominate in the presence of high Yb^{3+} ion concentration. This is supported by the power dependence for the silica thin film made with $La_{0.90}Yb_{0.05}Er_{0.05}F_3$ nanoparticles (Figure 8a), which shows the appearance of a feedback point at lower laser density (~94 W/cm^2) relative to thin films (Figure 8b) made with $La_{0.45}Lu_{0.50}Er_{0.05}F_3$ nanoparticles (~125 W/cm^2). We note, however, that, in our proposed mechanism, changing the Yb^{3+} concentration simultaneously affects the efficiency of ETU (Figure 7a) and the feedback loop (Figure 7b), both of which influence the onset of the feedback point.

Our previous report[15] showed the presence of a nonstoichiometric lanthanum silicate phase ($La_{9.31}Si_{6.24}O_{26}$) along with the expected LaF_3 phase from X-ray diffraction (XRD) studies carried out on a silica thin film sample heated at 800 °C. It is reasonable to assume that the same phases are present in the current sample reported in this report because they were prepared similarly. It is, however, important to know in which phase the hetero-LEET mechanism occurs. Two control samples have been prepared to investigate this. Citrate-stabilized $La_{0.45}Yb_{0.50}Er_{0.05}F_3$ and $La_{0.45}Lu_{0.50}Er_{0.05}F_3$ nanoparticles have been heated to burn off the citrate, and XRD data on these materials confirm the presence of pure LaF_3 phase. The power dependence graph of the heated $La_{0.45}Yb_{0.50}Er_{0.05}F_3$ control material (Figure 9a) is also S-shaped, similar to the power dependence graph of the silica thin film made with $La_{0.45}Yb_{0.50}Er_{0.05}F_3$ nanoparticles. It demonstrates that the slopes of both the red and green emission increase rapidly with increasing excitation power, giving a maximum slope of ~6. This strongly indicates that the hetero-LEET mechanism happens in the LaF_3 phase and also that the apparent many-photon power dependence is not an artifact due to the presence of impurities or multiple phases. We note that the maximum slope in the $La_{0.45}Yb_{0.50}Er_{0.05}F_3$ control sample is lower than that in the silica thin film made with $La_{0.45}Yb_{0.50}Er_{0.05}F_3$ nanoparticles. This may be due to the involvement of the silicate phase in the hetero-LEET mechanism, but it could also be simply due to the interaction of the Ln^{3+} ions near the surface of the nanoparticles with the silica matrix. Because of the high surface-to-volume ratio of these nanoparticles, the interaction of the nanoparticles with the host matrix has a significant effect on their luminescence properties.[15] Hence, the LaF_3 phase plays a major role in the hetero-LEET, but involvement of the silicate phase cannot be ruled out. Further studies to resolve this are in progress.

Conclusion

In conclusion, we report a new, potentially efficient up-conversion mechanism termed hetero-LEET for generation of green and red emission from silica thin films made with $La_{0.45}Yb_{0.50}Er_{0.05}F_3$ nanoparticles. This mechanism combines the advantages of resonant ground-state absorption and ETU with a cross-relaxation feedback loop that results in an *avalanche-like* power dependence.

Acknowledgment. The Natural Science and Engineering Research Council (NSERC) of Canada, the Canada Foundation for Innovation (CFI), and the British Columbia Knowledge Development Fund (BCKDF) of Canada are gratefully acknowledged for financial support. Acknowledgment is made to the Donors of the American Chemical Society Petroleum Research Fund for partial support of this research (P.S.M.).

JA065378X